# Calculation of $B(E2) \downarrow$, spectroscopic quadrupole moments $Q(J)$, and magnetic dipole moments $\mu(J)$ for the yrast states in $^{196}$Pt by a projection formalism

Sylvian Kahane*

*Physics Department, Nuclear Research Center—Negev, P.O. Box 9001, Beer-Sheva 84190, Israel*

K. H. Bhatt†

*Department of Physics and Astronomy, University of Mississippi, University, Mississippi 38677*

S. Raman‡

*Physics Division, Oak Ridge National Laboratory, Oak Ridge, Tennessee 37831*

The three major electromagnetic transition quantities, $B(E2) \downarrow$, $Q(J)$, and $\mu(J)$, are calculated for the yrast band of $^{196}$Pt by a projection formalism. The valence nucleon space is divided into four sectors of normal and abnormal parity states for neutrons and protons separately. The collective properties are evaluated in each of the four sectors and summed. A comparison is made with the IBM and SO(6) results, and it is shown that the projection calculations are performing equally well using only one fitted parameter and one normalization.

## I. INTRODUCTION

$^{196}$Pt is considered to exemplify the SO(6) limit of the interacting boson model (IBM) [1–3]. IBM is very successful in the interpretation of the $A = 180$–200 mass region (also known as the Pt-Os region) where a gradual change from the strongly deformed rare-earth nuclei and the spherical closed-shell Pb nucleus occurs, and where simple rotational or vibrational models are not adequate. Moreover, shape transitions are known to occur in this region, from prolate shapes for the lighter mass nuclei to oblate shapes for heavier ones. A wealth of experimental techniques have been applied to the study of $^{196}$Pt, including Coulomb excitation, neutron capture $(n, \gamma)$, and neutron inelastic scattering $(n, n' \gamma)$. These investigations resulted in a detailed and complex level scheme up to $E_x \approx 3$ MeV. The quadrupole moment of the first $2^+$ state was measured and found to be positive and, therefore, $^{196}$Pt is oblate.

In the SO(6) symmetry [1], the Hamiltonian eigenvalues are described by a three-parameter analytical expression:

$$E^{\text{SO(6)}}(\sigma, \tau, L) = A\sigma(\sigma + 4) + B\tau(\tau + 3) + CL(L + 1),$$
(1)

depending on the quantum numbers $\sigma$, $\tau$, and $L$ of the SO(6)⊃ SO(5)⊃SO(3) chain. Cizewski *et al.* [4] successfully fitted this formula to the low-lying states of $^{196}$Pt, thus providing evidence that this nucleus is a good example of the SO(6) symmetry. Moreover, in SO(6) not only the energy of the states can be calculated but also the $B(E2)$s of the transitions between those states and their quadrupole moments can be determined. The assumed form of the electric quadrupole

operator is

$$T^{E2} = e\hat{Q} = e([s^\dagger \times \tilde{d} + d^\dagger \times \tilde{s}]^{(2)} + \chi[d^\dagger \times d^\dagger]^{(2)}), \quad (2)$$

where $s$ and $d$ are the boson operators. In the strict SO(6) limit $\chi \equiv 0$, implying that all the quadrupole moments vanish. This expectation conflicts with the experimental results where a strong nonzero $Q(2_1^+)$ was measured. To solve this problem, Casten and Cizewski [5] proposed to perturb the strict SO(6) limit with a quadrupole-quadrupole interaction with the following Hamiltonian:

$$\mathcal{H} = E^{\text{SO(6)}} + \chi \hat{Q} \cdot \hat{Q}, \quad (3)$$

allowing in this way for nonzero values for $\chi$ while keeping the energies close to the SO(6) limit. Later, Fewell [6] proposed that, actually, the SU(5) limiting symmetry can give a good description of the $^{196}$Pt nucleus. In the recent work of Tavucku *et al.* [7] it was assumed that the SO(6) dynamical symmetry is broken and a full IBM-2 calculation was performed. In looking for the correct IBM-2 Hamiltonian parameters, those of the SO(6) symmetry were taken as the starting values. As expected, the final IBM-2 parameters were not too far from those SO(6) starting values.

In the present work we calculate the values for $B(E2)$s, electric quadrupole moments $Q(J)$, and magnetic dipole moments $\mu(J)$ in a projection formalism that is very distinct from the IBM philosophy.

IBM owes its phenomenal success to its ability to reduce the enormous configuration space of the shell model to a more restricted one of the boson model (and also taking advantage of symmetries). In the same spirit the projection model developed in Refs. [8,9] considers only the valence nucleons in a major shell and has a truncated configuration space compared with a full shell model calculation. To compensate for the neglected shells, one uses effective charges of a quite general form valid for all nuclei. (Note that the IBM also uses effective charges but they are adjusted for the nucleus being investigated.)

*Electronic address: skahane@bgumail.bgu.ac.il.
†Retired.
‡Deceased.

Moreover, the major shell configuration space is divided into four sectors, protons or neutrons, of normal or abnormal parity. In this way we address directly the problem of the contribution of abnormal parity states to the collectivity and deformation. This vexing issue was often bypassed in other models [e.g., pseudo-SU(3) or the fermion dynamic symmetric model] by assuming that the abnormal parity nucleons are coupled to $J = 0$ and their contribution to collectivity and deformation is zero or negligible. In contrast, we found in cases of synthetic nuclear structures, contributions as high as those of the normal parity nucleons coming from the abnormal parity nucleons.

Each one of the four sectors is described by an intrinsic state ($\mathcal{IS}$) in the form of a Slater determinant, constructed from single-particle deformed wave functions. States of good (collective) angular momentum are projected out from these $\mathcal{IS}$s. The contribution of a given sector to a collective property is obtained by considering its nucleons as active and nucleons from other sectors as spectators. For the normal parity sectors the pseudo-SU(3) symmetry is displayed by its nucleons. For the abnormal parity sectors the treatment is more complex and involves the decoupling of each nucleon from its $\mathcal{IS}$ (Slater determinant), calculation of a single-particle quantity (matrix element) in the presence of the other sector's nucleons, and summation over all the single-particle contributions.

To use the IBM model one cannot start with a totally unknown nucleus. A fairly detailed level scheme is necessary to fit the parameters of the IBM Hamiltonian and to establish its most probable (or closest) symmetry. In contrast, the projection procedure can be initiated with very minimal information, despite its large number of equations. Essentially, only the specific numbers of protons and neutrons are necessary to begin a calculation. Apart from the pseudo-SU(3) general symmetry for the normal parity nucleons, no particular per nucleus symmetries are implied or used. Also only a very light dependence on the specific form of parametrization is needed. These desirable features come at the price that the projection formalism, at present, is limited to the yrast states only, whereas the IBM is much more flexible, being able to calculate in-band and intraband transitions.

## II. FORMALISM

A projection formalism for even-even nuclei was developed in Refs. [8,9]. Only a brief recapitulation is given here. We consider only the valence nucleons in a major shell: for $^{196}$Pt this will be the 50–82 shell for protons and the 82–126 shell for neutrons. Each shell contains a number of states $|j_n\rangle$ with the same parity—the normal-parity ($n$) states—and an intruder state $|j_a\rangle$ with an opposite parity—the abnormal-parity ($a$) state. For $^{196}$Pt the $a$ states will be $0h_{\frac{11}{2}}$ for protons and $0i_{\frac{13}{2}}$ for neutrons. The number of valence nucleons is split accordingly into four subspaces: normal protons $N_{n\pi}$, abnormal protons $N_{a\pi}$, normal neutrons $N_{n\nu}$, and abnormal neutrons $N_{a\nu}$. Using Table VIII of Ref. [10] these numbers for $^{196}$Pt are 16, 12, 24, and 12, respectively.

### A. Intrinsic states ($\mathcal{IS}$)

In the prolate axially symmetric field of a deformed nucleus, each of the subspaces defined above is described by an intrinsic state ($\mathcal{IS}$) in the form of a single Slater determinant. For $N_n$ nucleons in the $n$ states we have

$$\mathcal{F}_{K_n}(N_n) = \left| \phi_{k_1}^{\alpha_1} \ \phi_{k_2}^{\alpha_2} \ \ldots \ \phi_{k_{N_n}}^{\alpha_{N_n}} \right|, \quad K_n = \sum_{i=1}^{N_n} k_i, \quad (4)$$

where $\phi_{k_i}^{\alpha_i}$ are deformed orbitals with $k = \langle j_z \rangle$, the projection of the angular momentum along the symmetry axis of the mean field. The labels $\alpha_i = 1, 2, \ldots$ distinguish different orbitals with the same $k_i$ value. $\phi_{k_i}^{\alpha_i}$ are asymptotically deformed in the configuration space of the $n$ states of the major shell. They are obtained from an asymptotically deformed Nilsson Hamiltonian and can be expanded in terms of the spherical $n$ states $\psi_{j_n k_i}$ as

$$\phi_{k_i}^{\alpha_i} = \sum_{j_n} c_{j_n k_i}^{\alpha_i} \psi_{j_n k_i}, \quad i = 1, 2, \ldots, N_n. \quad (5)$$

These orbitals are ordered sequentially by decreasing quadrupole moments

$$q_{k_i}^{\alpha_i} = \langle \phi_{k_i}^{\alpha_i} | q_0^2 | \phi_{k_i}^{\alpha_i} \rangle, \quad (6)$$

tabulated in Tables I–III of Ref. [8].

For $N_a$ nucleons in an $a$ state, the $\mathcal{IS}$ will be

$$\mathcal{F}_{K_a}(N_a) = \left| \psi_{j_a \frac{1}{2}} \ (-1)^{j_a - \frac{1}{2}} \psi_{j_a - \frac{1}{2}} \ \psi_{j_a \frac{3}{2}} \ \cdots \right.$$
$$\left. \times \ \psi_{j_a \frac{N_a}{2}} \ (-1)^{j_a - \frac{N_a}{2}} \psi_{j_a - \frac{N_a}{2}} \right|, \quad (7)$$

with $K_a = N_a/2$ for odd $N_a$ and $K_a = 0$ for even $N_a$. For the $a$ state there is a single intruder orbital and therefore only spherical states $\psi_{j_a k_i}$ appear in the $\mathcal{IS}$.

For the $a$ nucleons and oblate deformation, the occupied orbitals will be ordered by decreasing values of $k_i$ starting with $j_a$ (increasing values of the quadrupole moments):

$$\mathcal{F}_{K_a}(N_a) = \left| \psi_{j_a j_a} \ (-1)^{j_a - j_a} \psi_{j_a - j_a} \ \psi_{j_a (j_a - 1)} \ \cdots \right.$$
$$\left. \times \ \psi_{j_a (j_a - \frac{N_a}{2})} \ (-1)^{j_a - (j_a - \frac{N_a}{2})} \psi_{j_a -(j_a - \frac{N_a}{2})} \right|.$$
$$(8)$$

These $\mathcal{IS}$s of the four groups of nucleons are expanded in terms of the states $|J_\alpha (K_\alpha)\rangle$ of good angular momentum and projected from them

$$\mathcal{F}_{K_\alpha}(N_\alpha) = \sum_{J_\alpha} C_{J_\alpha K_\alpha} |J_\alpha (K_\alpha)\rangle, \quad (9)$$

with the label $\alpha$ standing for $n\pi, a\pi, n\nu$, and $a\nu$. The $C_{JK}$ coefficients are obtained by the projection procedure [8]

$$|C_{JK}|^2 = \frac{2J + 1}{2} \int d_{KK}^J(\beta) \langle \mathcal{F}_K(N) | e^{-i\beta J_y} | \mathcal{F}_K(N) \rangle \sin \beta d\beta, \quad (10)$$

where $d_{KK}^J(\beta)$ are the rotation functions.

The nucleons in $n$ states obey the pseudo-SU(3) symmetry. The yrast band of states with definite $J$ contained in the SU(3) representations $[\lambda, \mu]$ can be projected from the highest weight intrinsic state $\mathcal{F}[\lambda, \mu]$. An intrinsic state with $\mu \neq 0$

is triaxial in shape and contains different $K$ bands with $K = \mu, \mu - 2, \ldots 1$ or 0. We shall associate the yrast band with only the $K = 0$ band. This band contains the states $|J(K)\rangle$ with $J = 0, 2, 4, \ldots, \lambda + \mu$. The specific SU(3) $[\lambda, \mu]$ representations for a given $N_n$ are given in Table VIII of Ref. [10]. The $C_{JK}$ coefficients were calculated for the corresponding $[\lambda + \mu, 0]$ representation using the algebraic formula of Vergados [11]:

$$|C_{JK}(\lambda, 0)|^2 = \begin{cases} \dfrac{1}{\lambda + 1} & \text{for } J = 0, \\ (2J+1)\dfrac{\lambda(\lambda-1)(\lambda-2)\cdots(\lambda-J+1)}{(\lambda-J+1)(\lambda-J+3)\cdots(\lambda+J-1)(\lambda+J+1)} & \text{for } J \geqslant 1. \end{cases} \quad (11)$$

The above expressions are for standard prolate deformation. In $^{196}$Pt we get $[\lambda, \mu] = [2, 8]$ for normal protons and [6,12] for normal neutrons; therefore, the calculated $C_{J_n K_n}$ are for [10,0] and [18,0] representations, respectively.

The expansion coefficients for the $a$ nucleons $C_{J_a K_a}$ were calculated in Table II of Ref. [9] for an even number of nucleons $N_a = 2, 4, 6$, and 8 by direct integration of Eq. (10). In the $^{196}$Pt case there are 12 protons in $0h_{\frac{11}{2}}$ and 12 neutrons in $0i_{\frac{13}{2}}$. In the proton case, the intruder orbital is full $(2j + 1 = 12)$ and therefore $C_{J_a K_a} = 1.0$ for $J_a = 0$ and zero for the other values of $J_a$. For the neutron $(\frac{13}{2})^{12}$ configuration the $C_{J_a K_a}$ are given by the simple expressions $(K = 0)$

$$C_{JK}^2 = \begin{cases} 2\left(\frac{13}{2}\,\frac{13}{2}\,\frac{13}{2}\,-\frac{13}{2}\,\big|\,J\,0\right)^2 & \text{prolate,} \\ 2\left(\frac{13}{2}\,\frac{1}{2}\,\frac{13}{2}\,-\frac{1}{2}\,\big|\,J\,0\right)^2 & \text{oblate.} \end{cases} \quad (12)$$

The results for the prolate deformation are presented in Table I of this article and supplement the data of Ref. [9].

Using the $\mathcal{IS}$s defined above for the various sectors, a general formula for the electromagnetic transition matrix elements in a given sector is presented in Appendix A. The total matrix elements are a summation over the contributions of all four sectors. The formula is subsequently applied to the calculation of the electric quadrupole matrix elements in Appendix B and magnetic dipole ones in Appendix C.

TABLE I. Expansion coefficients $C_{JK}$ and reduced quadrupole matrix elements for $N_a = 12$ and $j_a = \frac{13}{2}$ in units of $\alpha^2$.

| $J$ | $|C_{JK}|^2$ | $\langle J'\|\hat{Q}\|J\rangle$ | |
|---|---|---|---|
| | | $J \to J$ | $J+2 \to J$ |
| 0 | 0.142857 | 0.0 | 14.8842 |
| 2 | 0.464286 | $-16.5493$ | 22.6309 |
| 4 | 0.300420 | $-16.2303$ | 25.7350 |
| 6 | $0.822203 \times 10^{-1}$ | $-10.0750$ | 25.3569 |
| 8 | $0.977444 \times 10^{-2}$ | 2.8694 | 21.5442 |
| 10 | $0.437475 \times 10^{-3}$ | 23.3451 | 14.0948 |
| 12 | $0.480741 \times 10^{-5}$ | 52.0483 | |

### B. $B(E2)$s and the spectroscopic quadrupole moments

A discussion on the matrix elements of the electric quadrupole operator is given in Appendix B. The $B(E2)$s are calculated from the nondiagonal matrix elements as follows:

$$B(E2: J(K) \to J'(K)) = \frac{5}{16\pi}\frac{\langle J'(K)\|\hat{Q}_e\|J(K)\rangle^2}{2J+1}, \quad (13)$$

whereas the spectroscopic quadrupole moments are obtained from the diagonal ones as follows:

$$Q(J) = \frac{(J\,J\,2\,0\,|\,J\,J)}{\sqrt{2J+1}}\langle J\|\hat{Q}_e\|J\rangle. \quad (14)$$

### C. Magnetic moments

For the calculation of the magnetic dipole operator matrix elements, we use only three sectors: two abnormal parity sectors for the protons and neutrons, and one normal parity sector including both the neutrons and protons. This approach is dictated by the assumed form of the magnetic dipole operator matrix elements in the normal parity sector. Detailed formulas are given in Appendix C.

The total magnetic moment is obtained as a summation over the three sectors as follows:

$$\mu(J(K)) = \mu_{a\pi}(J(K)) + \mu_{av}(J(K)) + \mu_n(J(K)). \quad (15)$$

The parameter $g_n$ (see Appendix C) was fixed by looking for the best agreement with experimental data.

### D. Simulating oblate shapes

$^{196}$Pt is considered oblate on the basis of the sign of its $Q(2_1^+)$ quadrupole moment. The oblateness will manifest itself via the reduced matrix elements $\langle J'_\alpha(K_\alpha)\|T_\alpha^{(\lambda)}\|J_\alpha(K_\alpha)\rangle$ between the states $|J_\alpha(K_\alpha)\rangle$ projected from the $\mathcal{IS}$ of the $N_\alpha$ nucleons and, additionally, in Eq. (A4) via the coupling coefficients $A[JK; J_\alpha K_\alpha; J_s K_s]$ that depend on the expansion coefficients $C_{JK}$, which are different for the prolate and oblate configurations.

In the present formalism oblate calculations for $\langle J'_\alpha(K_\alpha)\|\widehat{E2}\|J_\alpha(K_\alpha)\rangle$ can be performed for the $a$ nucleons using Eqs. (8), (12), and (B5). As is evident from the formulas

of Appendix C there is no prolate-oblate dependence for the $\langle J'_\alpha(K_\alpha) \| \widehat{M1} \| J_\alpha(K_\alpha) \rangle$ matrix elements.

By extensive numerical calculations, we found that the quadrupole operator reduced matrix elements (RMEQ) for the $a$ nucleons have the following symmetry relations:

$$\text{RMEQ}^{\text{prolate}}(N_a) = -\text{RMEQ}^{\text{oblate}}(2j_a + 1 - N_a). \quad (16)$$

These relations imply in particular that for a half-filled shell, that is, $N_a = (2j_a + 1)/2$, the oblate RMEQ will be exactly the prolate RMEQ with a change of sign. For the $n$ nucleons there is not a corresponding oblate formalism. Taking the cue from the behavior of the $a$ nucleons, the total oblate reduced matrix elements for the $N_n + N_a$ nucleons [i.e., those calculated with Eq. (A4)] are *approximated* as follows:

$$\text{RMEQ}^{\text{oblate}}(N_n + N_a) = -\text{RMEQ}^{\text{prolate}}(N_n + N_a). \quad (17)$$

This change of sign has no influence on the $B(E2)$ calculations because of their dependence on the square of the matrix elements, but it will influence the sign of the quadrupole moments that depend on the matrix elements directly.

For the magnetic case, the total oblate reduced matrix elements were *approximated* to be exactly those given by the prolate calculations (this amounts to neglecting the oblate dependence in the $A$ coefficients).

### III. RESULTS

#### A. $B(E2: J \to J - 2)$

The quadrupole matrix elements are symmetric for transitions between states differing by two units of angular momentum, that is, $\langle J_f \| \hat{Q}_e \| J_i \rangle = \langle J_i \| \hat{Q}_e \| J_f \rangle$; then Eq. (13) implies in particular

$$B(E2: J \to J - 2) = B(E2: (J - 2) \to J) \frac{2(J-2)+1}{2J+1}. \quad (18)$$

Experimental values for $B(E2: (J - 2) \to J)$ were taken from Ref. [12] for the ground state band, producing the $B(E2: J \to J - 2)$ values shown in Table II. The uncertainities were calculated assuming the maximum additive scenario, that is, when a value is given as $0.658 + 29 - 69$ it was interpreted as $0.658 \pm 0.098$.

We show in Table II projected $B(E2)$ calculations for the full length of the yrast band projected from the $\mathcal{IS}$, and also calculations based on the SO(6) symmetry of the IBM Hamiltonian and of a full IBM-2 Hamiltonian. In the latter calculation, no particular symmetry was assumed but rather the IBM-2 Hamiltonian was fitted to the experimental level scheme. The IBM-2 and SO(6) calculations were taken from the works of Tavucku *et al.* [7] and Van Isacker [13]. Both the projected and the IBM-2 calculations are normalized to the first $B(E2: 2^+ \to 0^+)$ experimental value. For the SO(6) normalization, see the next subsection. In Figs. 1(a) and 1(b) we show these results graphically. It can be seen from Fig. 1(b) that the projected calculations are doing somewhat better than both the SO(6) and IBM-2 calculations. The experimental value at $J = 8$ seems to imply a stronger

TABLE II. Experimental and calculated values of $B(E2: J \to J - 2)$ (in $e^2\text{b}^2$) for the yrast band in $^{196}$Pt.

| | | Calculations | | |
| --- | --- | --- | --- | --- |
| $J$ | Experimental values | Projected | IBM-2 | SO(6) |
| 2 | $0.274 \pm 0.0012$ | 0.274 | 0.274 | 0.286 |
| 4 | $0.405 \pm 0.006$ | 0.389 | 0.361 | 0.374 |
| 6 | $0.455 \pm 0.067$ | 0.424 | 0.366 | 0.381 |
| 8 | $0.532 \pm 0.107$ | 0.438 | | |
| 10 | | 0.441 | | |
| 12 | | 0.438 | | |
| 14 | | 0.430 | | |
| 16 | | 0.418 | | |
| 18 | | 0.403 | | |
| 20 | | 0.385 | | |
| 22 | | 0.365 | | |
| 24 | | 0.341 | | |
| 26 | | 0.314 | | |
| 28 | | 0.285 | | |
| 30 | | 0.253 | | |
| 32 | | 0.218 | | |
| 34 | | 0.180 | | |
| 36 | | 0.139 | | |
| 38 | | 0.095 | | |
| 40 | | 0.048 | | |

collectivity than predicted by any of the model calculations. This particular measurement has a great uncertainty and, therefore, this conclusion is questionable.

#### B. Spectroscopic quadrupole moments Q(J)

Calculations for the spectroscopic quadrupole moments are presented in Fig. 2 and Table III. Experimental data for the $2^+_1$, $4^+_1$, and $6^+_1$ levels were taken from Lim *et al.* [14], Gyapong *et al.* [15], and Mauthofer *et al.* [16].

We also show the SO(6) calculations of Van Isacker [13]. The SO(6) functional forms for the $B(E2)$ and $Q(J)$ are $f(N)e^2\chi^2$ and $g(N)e\chi$, respectively. $f(N)$ and $g(N)$ are algebraic functions of the number of bosons $N$ (6 in the case of $^{196}$Pt), whereas $e$ (the effective boson charge) and $\chi$ are IBM parameters. The boson effective charge $e$ was obtained from the $B(E2: 2^+_1 \to 0^+_1)$ as $0.152\, e$ b, and $\chi$ was chosen to be 0.580 to fit experimental data, which contained four $B(E2)$ and one $Q(2^+_1)$ values. The $B(E2)$ values are not sensitive to the sign of $\chi$ because of their $\chi^2$ dependence. $\chi$ was chosen to be positive on the basis of the experimental $Q(2^+_1)$ value [$f(N)$ and $g(N)$ have positive values]. In this respect the SO(6) calculations do not have a too much predictive power, but rather they were fitted to give resonable results.

From Fig. 2 it is quite obvious that the values for the $4^+_1$ and $6^+_1$ levels are not solid. At $4^+_1$ there are two measurements in strong disagreement and at $6^+_1$ there are two measurements with large error bars. Only for the $2^+_1$ level are the measurements of Lim *et al.* and Gyapong *et al.* close and consistent, giving a solid positive value. Overall the quadrupole moments data seem to be decreasing with the $J$ increase, a trend reproduced by the projected calculations, but contradicting the
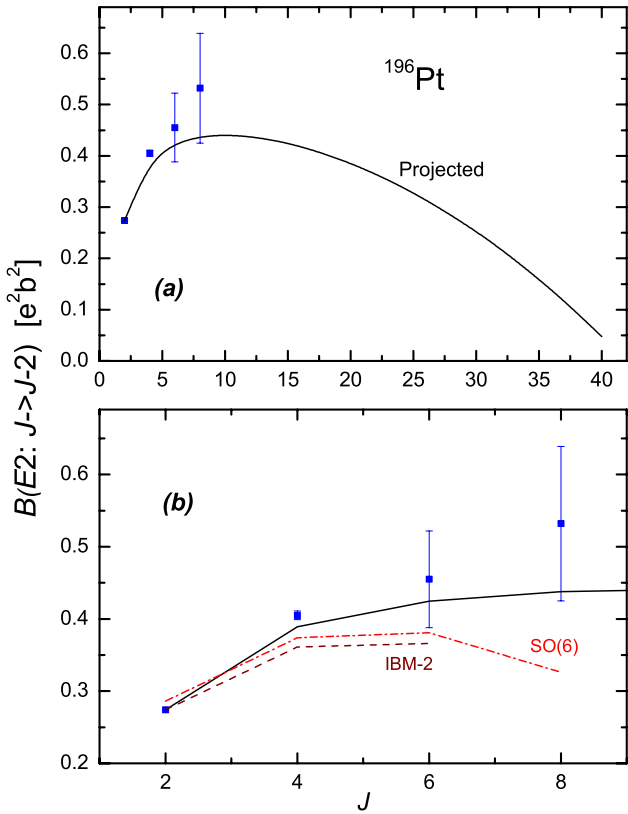
FIG. 1. (Color online) (a) Projected calculation for the full yrast band vs experimental $B(E2 : J \to J - 2)$ values in $^{196}$Pt. (b) As above, only for the region of existing experimental data. The shown SO(6) and IBM-2 calculations are taken from Tavucku *et al.* [7] for the $2^+_1$, $4^+_1$, and $6^+_1$ states, and from Van Isacker [13] for the $8^+_1$ state.

SO(6) calculations which are increasing, at least for the limited range $2^+_1 \to 6^+_1$. In view of the approximations made to get the oblate RMEQ, the excellent agreement of the experimental $Q(2^+_1)$ and the projected calculation is quite fortuitous.

TABLE III. Calculated values of $Q(J)$ and $\mu(J)$ for the yrast band in $^{196}$Pt.

| $J$ | $Q(J)$ (b) | $\mu(J)$ (nm) |
|-----|-----------|---------------|
| 2   | 0.61993   | 0.84266       |
| 4   | 0.58749   | 1.256         |
| 6   | 0.53683   | 1.5674        |
| 8   | 0.49304   | 1.8272        |
| 10  | 0.45673   | 2.0544        |
| 12  | 0.42633   | 2.2587        |
| 14  | 0.40042   | 2.4457        |
| 16  | 0.37792   | 2.619         |
| 18  | 0.35802   | 2.7809        |
| 20  | 0.34012   | 2.9334        |
| 22  | 0.32375   | 3.0776        |
| 24  | 0.30852   | 3.2144        |
| 26  | 0.2941    | 3.3447        |
| 28  | 0.28017   | 3.4689        |
| 30  | 0.26641   | 3.5872        |
| 32  | 0.25241   | 3.6998        |
| 34  | 0.23768   | 3.8065        |
| 36  | 0.22138   | 3.9068        |
| 38  | 0.20209   | 3.9993        |
| 40  | 0.17674   | 4.0813        |

We calculated the curve labeled IBM-3 in Fig. 2 by using the Hamiltonian parameters given by Tavucku *et al.* [7] and the NPBTRN program of Otsuka. Unlike the positive $\chi$ value used by Van Isacker [13], Tavucku *et al.* [7] fixed $\chi$ at a negative value of $-0.036$, forcing negative values for the spectroscopic quadrupole moments [IBM-2 calculations being close to the SO(6), the above observations on the SO(6) dependence on $\chi$ apply], missing the oblate character of $^{196}$Pt. The notation IBM-3 stresses that these are not the original IBM-2 calculations of Tavucku *et al.*, hence any mistakes are our responsibility. For this calculation one has to use boson
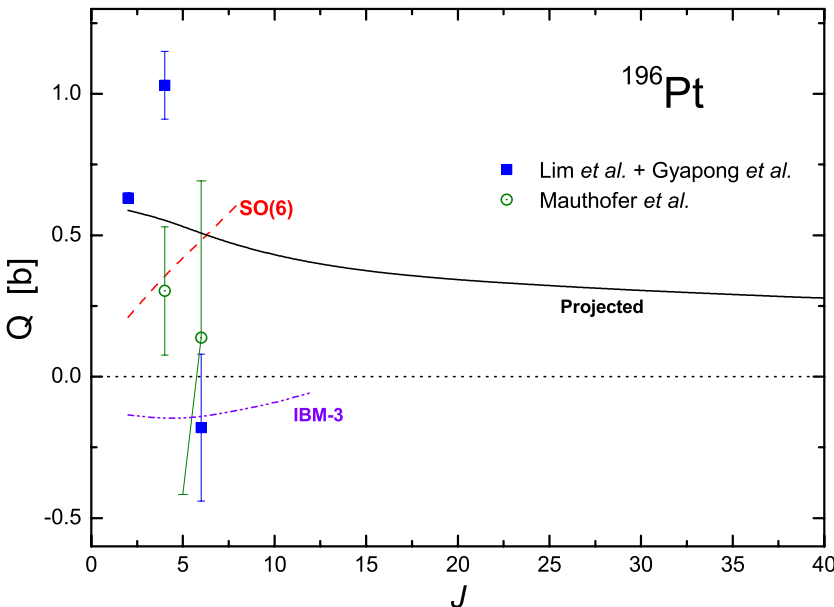


FIG. 2. (Color online) Projected calculation of the quadrupole spectroscopic moment for the yrast band in $^{196}$Pt. Experimental points are taken from Lim *et al.* [14] (solid squares) (averaged with Gyapong *et al.* [15] at $2^+_1$) and from Mauthofer *et al.* [16] (hollow circles). The SO(6) calculation is from Van Isacker [13]. The curve labeled IBM-3 is an IBM-2 calculation based on the Hamiltonian of Tavucku *et al.* [7] and the effective boson charges of Van Isacker.
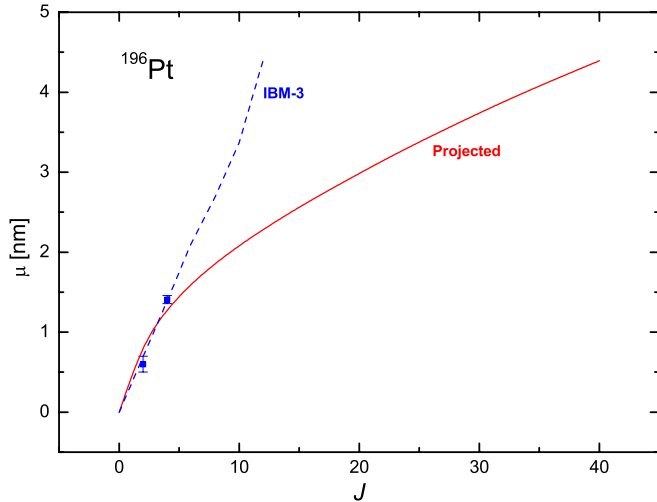
FIG. 3. (Color online) Projected calculation of the magnetic dipole moment for the yrast band in $^{196}$Pt. The experimental value at $2_1^+$ is an average of Refs. [17–20], whereas the value at $4_1^+$ is an average of values from Refs. [21,22]. The value of the parmeter $g_n$ was fixed at 1.4. The IBM-3 curve was calculated as in Fig. 2 with the g factors $g_n = 0.1$ and $g_p = 0.9$.

effective charges that were also taken from Tavucku *et al.* [7], namely 0.154 *e* b for both *s* and *d* bosons.

### C. Magnetic moments $\mu(J)$

The only measured magnetic moments are for the $2_1^+$ and $4_1^+$ states. The experimental data were taken from Refs. [17–22]. Projected calculations are presented in Fig. 3 and Table III. To obtain fair agreement, the parameter $g_n$ was chosen as 1.4. The contribution of the abnormal protons is zero because the $0h_{\frac{11}{2}}$ orbital is filled, the abnormal neutrons give a negative contribution, and the $n$ nucleons a positive one.

The curve IBM-3 was explained in the previous subsection. Here there are two free parameters, the g factors, enabling a perfect fit to the only two existing measurements. We used $g_n = 0.1$ and $g_p = 0.9$. The IBM model predicts a much stronger collectivity, at higher spins, compared with the projected calculations. The available data do not permit us to choose between the two models.

### IV. CONCLUSIONS

This work presented a projected formalism calculation of the collective properties of $^{196}$Pt and compared them with existing experimental data and with IBM calculations. The IBM is heavily dependent on parametrization, both in the Hamiltonian and in the calculated quantities like $B(E2)$ and $Q(J)$, as was discussed above. In contrast, the projected calculations are loosely dependent on parametrization. There is a dependence on quite general forms of the effective charges and effective orbital and spin g factors, and the SU(3) and single particle quadrupole matrix elements are calculated with harmonic oscillator wave functions. All these are general and not specific to any nucleus. The only true parameter of the calculations is $g_n$ used for the magnetic moment and, to a lesser

degree, the renormalization of the $B(E2)$s to the experimental $B(E2 : 2_1^+ \rightarrow 0_1^+)$. In view of this light parameter dependence, the projected calculations are performing very well.

### APPENDIX A: MATRIX ELEMENTS IN A GIVEN SECTOR

To calculate the contribution of each group $\alpha$ of nucleons to the quadrupole moments, $B(E2)$s and other collective properties we note that than only the $N_\alpha$ nucleons contribute actively to the matrix elements, while the remaining nucleons influence the matrix elements only as Racah spectators. The $\mathcal{IS}$ for the whole nucleus is

$$\mathcal{F}_K(N) = \mathcal{F}_{K_\alpha}(N_\alpha)\mathcal{F}_{K_s}(N_s), \qquad (A1)$$

where $\alpha$ stands for the group of nucleons in question and $s$ stands for the rest of the nucleus (spectators). The rest of the nucleus is considered to be described by a SU(3) $[\lambda_s, 0]$ representation with $\lambda_s = \sum_\beta \lambda_\beta$ where $\beta$ runs on the other three groups of nucleons different from $\alpha$. This *ansatz* rests on the observation made in Table III of Ref. [9] that even for *a*-parity nucleons groups, there are *equivalent* SU(3) representations $\lambda_{eq} = J_{amax}$ describing very well the angular momentum content of their $\mathcal{IS}$: $N_s = \sum_\beta N_\beta$, $N = N_\alpha + N_s$ and similarly for $K$.

The above $\mathcal{IS}$ for the whole nucleus is expanded in projected states of good angular momentum

$$\mathcal{F}_K(N) = \sum_J C_{JK}|J(K)\rangle,$$

$$|C_{JK}|^2 = (N_{JK})^{-2},$$

$$N_{JK} = \left[ \sum_{J_\alpha}\sum_{J_s} |C_{J_\alpha K_\alpha}(N_\alpha)C_{J_s K_s}(N_s) \right.$$

$$\left. \times (J_\alpha K_\alpha J_s K_s | J K)|^2 \right]^{-1/2}, \qquad (A2)$$

where $C_{J_s K_s}$ are calculated for the SU(3) $[\lambda_s, 0]$ representation with the Vergados formula given in Eq. (11). We further define the expansion coefficients

$$A[JK; J_\alpha K_\alpha; J_s K_s] = N_{JK} C_{J_\alpha K_\alpha}(N_\alpha)C_{J_s K_s}(N_s)$$
$$\times (J_\alpha K_\alpha J_s K_s | J K). \qquad (A3)$$

The matrix elements of an operator $T_\alpha^{(\lambda)}$ of multipolarity $\lambda$ [not to be confused with the $\lambda$ used to specify the SU(3) representations], acting on the $N_\alpha$ nucleons of type $\alpha$, between the projected states $|J(K)\rangle$ of the whole nucleus, are obtained using Eq. (1A-72a) of Bohr and Mottelson [23] for coupled systems

$$\langle J'(K)\|T_\alpha^{(\lambda)}\|J(K)\rangle = \sqrt{(2J'+1)(2J+1)}$$

$$\times \sum_{J'_\alpha}\sum_{J'_s}\sum_{J_\alpha}\sum_{J_s} A[J'K; J'_\alpha K_\alpha; J'_s K_s]$$

$$\times A[JK; J_\alpha K_\alpha; J_s K_s]\Big[(-1)^{J'_\alpha + J'_s + J + \lambda}$$

$$\times \begin{Bmatrix} J_\alpha & J_s & J \\ J' & \lambda & J'_\alpha \end{Bmatrix} \langle J'_\alpha(K_\alpha)\|T_\alpha^{(\lambda)}\|J_\alpha(K_\alpha)\rangle \delta_{J'_s J_s}\Big]. \quad (A4)$$

reducing the problem to the calculation of matrix elements of the $T_\alpha^{(\lambda)}$ operator between the projected states $|J_\alpha(K_\alpha)\rangle$ of the $N_\alpha$ nucleons only.

## APPENDIX B. ELECTRIC QUADRUPOLE OPERATOR

When $T_\alpha^{(\lambda)}$ is the quadrupole operator, $\lambda = 2$, and $T^{(2)} = \hat{Q}_e$, with

$$\hat{Q}_e = \sqrt{\frac{16\pi}{5}} \sum_{i=1}^{N_\alpha} r_i^2 Y_0^2(\theta_i, \phi_i). \tag{B1}$$

We distinguish two cases:

1. If $\alpha$ specifies an $n$-parity group ($n\pi, n\nu$), then the matrix elements are proportional to the following SU(3) matrix elements

$$\langle J_\alpha'(K_\alpha)\|\hat{Q}_\alpha\|J_\alpha(K_\alpha)\rangle = 1.2\langle[\lambda_\alpha,0]J_\alpha'\|\hat{Q}_\alpha\|[\lambda_\alpha,0]J_\alpha\rangle, \tag{B2}$$

where $[\lambda_\alpha, 0]$ is the SU(3) representation with $\lambda_\alpha = J_{\alpha\,\text{max}}$ the maximum angular momentum for the $N_\alpha$ nucleons. The proportionality factor 1.2 was derived in Ref. [24]. The SU(3) matrix elements have the simple form [11] (in units of $\alpha^2 = 0.0101A^{1/3}$ the harmonic oscillator parameter)

$$\langle[\lambda,0]J'\|\hat{Q}\|[\lambda,0]J\rangle$$
$$= \begin{cases} 2\sqrt{(2J+1)}(J\,0\,2\,0|J\,0)\langle J\|r^2\|J\rangle & \text{for } J' = J \\ -2\sqrt{(2J+1)}(J\,0\,2\,0|J-2\,0)\times \\ \quad \langle J-2\|r^2\|J\rangle & \text{for } J' = J-2 \end{cases} \tag{B3}$$

with

$$\langle J'\|r^2\|J\rangle = \begin{cases} 2n + J + \frac{3}{2} & \text{for } J' = J \\ -2\sqrt{(n+1)(n+J+\frac{1}{2})} & \text{for } J' = J-2 \end{cases} \tag{B4}$$

where $n = (\lambda - J)/2$.

2. If $\alpha$ specifies an $a$-parity group, then one has to decouple the single-particle states from the Slater determinat of the $\mathcal{IS}$ Eq. (7), calculate the single-particle contributions, and sum over all the $N_a$ particles. This procedure was first outlined by Gunye and Warke [25] and was discussed also by Hara and Sun [26]. We applied it to our specific projection procedure and it appears as Eq. (75) in Ref. [9]. It is reproduced here for completeness:

$$\langle(j_a, N_a); J'K\|\hat{Q}\|(j_a, N_a); JK\rangle$$
$$= \sqrt{\frac{(2J'+1)(2J+1)}{C_{J'K}C_{JK}}} \sum_{i=1}^{N_a}\sum_{m=1}^{N_a}\sum_I (-1)^{i+m+j_i+J'+I+2}$$
$$\times c_{j_m\Omega_m}(K)c_{j_i\Omega_i}(K)p_{K-\Omega_m,K-\Omega_i}^I(N_a-1)$$
$$\times (I, K-\Omega_m; j_m, \Omega_m|J'K)\,(I, K-\Omega_i; j_i, \Omega_i|JK)$$
$$\times \begin{Bmatrix} J & j_i & I \\ j_m & J' & 2 \end{Bmatrix} (n_m l_m j_m\|q\|n_i l_i j_i). \tag{B5}$$

The sums over $i$ and $m$ run over the nucleons in the initial and final $\mathcal{IS}$s. The index $I$ is the angular momentum of the $N_a - 1$ spectator nucleons in the $\mathcal{IS}$ when one of the nucleons

is contributing to the reduced matrix element. The quantity $c_{j_i\Omega_i}(K)$ is the amplitude that the contributing nucleon in the initial state has an angular momentum $j_i$ and projection $\Omega_i$ [see Eq. (5)]. Similarly, $c_{j_m\Omega_m}(K)$ is the corresponding amplitude for the nucleon in the final $\mathcal{IS}$. In our calculation, $K = 0$ and $j_i = j_m = j_a$. The amplitudes are $c_{j_i,|\Omega_i|} = 1$ and $c_{j_i,-|\Omega_i|} = (-1)^{j_i-|\Omega_i|}c_{j_i,|\Omega_i|}$. The quantity $p_{K-\Omega_m,K-\Omega_i}^I(N_a-1)$ is the probability amplitude that the $N_a - 1$ spectator nucleons in the initial and final $\mathcal{IS}$s are coupled to a total angular momentum $I$, and it is given by

$$p_{K-\Omega_m,K-\Omega_i}^I(N_a-1)$$
$$= \langle \mathcal{F}_{K-\Omega_m}(j_a, N_a-1)|P_{K-\Omega_i}^I|\mathcal{F}_{K-\Omega_i}(j_a, N_a-1)\rangle, \tag{B6}$$

where $\mathcal{F}_{K-\Omega}(j_a, N_a-1)$ is the $\mathcal{IS}$ of the $N_a - 1$ spectator nucleons when the decoupled nucleon has a projection $\Omega$, and $P_K^I$ is the projection operator

$$P_K^I \mathcal{F}_K = C_{IK}|J(K)\rangle, \tag{B7}$$

producing states of good angular momentum $|J(K)\rangle$ out of the $\mathcal{IS}$. The Clebsch-Gordan coefficients in Eq. (B5) [written in the convention $(j_1, m_1; j_2, m_2|JM)$] represent the coupling between the $N_a - 1$ spectators and the contributing nucleon. The matrix elements of the single-particle electric quadrupole operator $q_\mu = \sqrt{16\pi/5}r^2Y_\mu^2$ are evaluated with the radial quantum numbers $n_i = n_m = 0$ and the orbital angular momenta $j_i = j_m = j_a - \frac{1}{2}$.

The calculation is complex and involves applying the projection procedure to all the minors of the determinant specifying the $\mathcal{IS}$. Results of the matrix elements in the abnormal parity sector for $N_a = 2, 4, 6$, and 8 particles were presented in Table XIII of Ref. [9]. The procedure was prone to numerical roundoff errors and, therefore, the calculations were performed analytically using MAPLE. The evaluation times were prohibitively long, making unfeasible calculations beyond the $N_a = 8$ particles.

In the $^{196}$Pt case there are 12 particles in $h_{\frac{11}{2}}$ and 12 particles in $i_{\frac{13}{2}}$. Because the $h_{\frac{11}{2}}$ orbital is full, the particles can couple only to $J = 0$ and the corresponding matrix element $\langle 0\|\hat{Q}\|0\rangle = 0$, that is, there is no deformation due to the abnormal protons. For the neutron case we employed a new numerical procedure based on Bailey's [27] multiprecision package. It was found sufficient to use the double-double precision (i.e., each variable is allocated 128 bits; same as in a Cray machine) to obtain numerically stable and accurate results. The prolate deformation calculations are presented in Table I and supplement those of Table XIII in Ref. [9].

The total quadrupole matrix elemets are calculated from the individual contributions of the four nucleon groups as follows:

$$\langle J'(K)\|\hat{Q}_e\|J(K)\rangle = \sum_\alpha e_\alpha\langle J'(K)\|\hat{Q}_\alpha\|J(K)\rangle \tag{B8}$$

with the effective charges $e_\pi = [1 + (Z/A)]e$ and $e_\nu = 2.1(Z/A)e$ for both the $n$ and $a$ nucleons. The individual

contributions in the right-hand side above are calculated with Eq. (A4).

### APPENDIX C: MAGNETIC DIPOLE OPERATOR

For the $a$-parity nucleons ($\alpha = a\pi$, $a\nu$), the reduced matrix elements of the $\widehat{M1}$ operator are given exactly [28] as

$$\langle J'_\alpha(K_\alpha)\|\widehat{M1}_\alpha\|J_\alpha(K_\alpha)\rangle$$
$$= \sqrt{\frac{3}{4\pi}} g_{j\alpha}\sqrt{J_\alpha(J_\alpha+1)(2J_\alpha+1)}\delta_{J'_\alpha,J_\alpha} \qquad (C1)$$

in units of nuclear magnetons $\mu_N = e\hbar/(2M_pc)$. The gyro-magnetic ratio is given by

$$g_j = \frac{1}{2j(j+1)}\left\{g_l\left[j(j+1)+l(l+1)-\frac{3}{4}\right]\right.$$
$$\left.+g_s\left[j(j+1)-l(l+1)+\frac{3}{4}\right]\right\} \qquad (C2)$$

with the orbital and spin $g$ factors $(g_l, g_s) = (1, 5.58)$ for free protons and $(0, -3.82)$ for free neutrons. The spin $j = j_a$ is the spin of the intruder orbital. In this work we used the effective orbital and spin $g$ factors $(g_{l\,\text{eff}}, g_{s\,\text{eff}}) = (g_l, 0.7g_s)$.

For the $n$-parity nucleons we can assume only that the magnetic dipole operator is proportional to the angular momentum operator $\hat{J}_n$:

$$\widehat{M1}_n = \sqrt{\frac{3}{4\pi}} g_n\hat{J}_n \qquad (C3)$$

giving the reduced matrix elements

$$\langle J'_n(K_n)\|\widehat{M1}_n\|J_n(K_n)\rangle$$
$$= \sqrt{\frac{3}{4\pi}} g_n\sqrt{J_n(J_n+1)(2J_n+1)}\delta_{J'_n,J_n}, \qquad (C4)$$

which formally resemble Eq. (C1), but here $g_n$ is a free parameter with no special meaning.

The nucleon space is divided into only three sectors: abnormal protons ($a\pi$), abnormal neutrons ($a\nu$), and normal parity nucleons (including the normal protons *and* the normal neutrons) ($n$), making the calculations dependent on only one parameter ($g_n$). The magnetic moment for a given sector is

$$\mu_\alpha(J(K)) = \sqrt{\frac{4\pi}{3}}(J\,J\,1\,0\,|\,J\,J)\frac{\langle J(K)\|\widehat{M1}_\alpha\|J(K)\rangle}{\sqrt{2J+1}}, \qquad (C5)$$

with the right-hand reduced matrix elements calculated from Eq. (A4).

[1] A. Arima and F. Iachello, Ann. Phys. (NY) **123**, 468 (1979).
[2] J. A. Cizewski *et al.*, Phys. Rev. Lett. **40**, 167 (1978).
[3] R. F. Casten and J. A. Cizewski, Phys. Lett. **B185**, 293 (1987).
[4] J. A. Cizewski *et al.*, Nucl. Phys. **A323**, 349 (1979).
[5] R. F. Casten and J. A. Cizewski. Nucl. Phys. **A309**, 477 (1978).
[6] M. P. Fewell, Phys. Lett. **B167**, 6 (1986).
[7] E. Tavukcu *et al.*, Phys. Rev. C **65**, 064309 (2002).
[8] S. Kahane, S. Raman, and K. H. Bhatt, Phys. Rev. C **55**, 2885 (1997).
[9] K. H. Bhatt, S. Kahane, and S. Raman, Phys. Rev. C **61**, 034317 (2000).
[10] K. H. Bhatt, C. W. Nestor, Jr., and S. Raman, Phys. Rev. C **46**, 164 (1992).
[11] J. D. Vergados, Nucl. Phys. **A111**, 687 (1968).
[12] Z. Chunmei, W. Gongqing, and T. Zhenlan, Nucl. Data Sheets **83**, 145 (1998).
[13] P. Van Isacker, Nucl. Phys. **A465**, 497 (1987).
[14] C. S. Lim, R. H. Spear, M. P. Fewell, and G. J. Gyapong, Nucl. Phys. **A548**, 308 (1992).
[15] G. J. Gyapong *et al.*, Nucl. Phys. **A458**, 165 (1986).

[16] A. Mauthofer *et al.*, Z. Phys. **336**, 263 (1990).
[17] A. E. Stuchbery, G. J. Lampard, and H. H. Bolotin, Nucl. Phys. **A528**, 447 (1991).
[18] R. Tanczyn *et al.*, Phys. Rev. C **48**, 140 (1993).
[19] R. Levy *et al.*, Phys. Rev. C **25**, 293 (1982).
[20] O. Häusser, B. Haas, D. Ward, and H. R. Andrews, Nucl. Phys. **A314**, 161 (1979).
[21] F. Brandolini *et al.*, Nucl. Phys. **A536**, 366 (1992).
[22] A. E. Stuchbery, C. G. Ryan, I. Morrison, and H. H. Bolotin, Phys. Rev. C **24**, 2106 (1981).
[23] A. Bohr and B. Mottelson, *Nuclear Structure* (Benjamin, New York, 1969), Vols. I and II.
[24] O. Castanõs, J. P. Draayer, and Y. Leschber, Ann. Phys. (NY) **180**, 290 (1987).
[25] M. R. Gunye and C. S. Warke, Phys. Rev. **159**, 885 (1967).
[26] K. Hara and Y. Sun, Int. J. Mod. Phys. E **4**, 637 (1995).
[27] D. H. Bailey, *A Fortran-90 Based Multiprecision System*, NASA Ames RNR Technical Report RNR-94-013 (1995).
[28] A. de-Shalit and I. Talmi, *Nuclear Shell Theory* (Academic, New York, 1963).